Chemical Science

EDGE ARTICLE

Helix-constructed polar rare-earth iodate fluoride as a laser nonlinear optical multifunctional material†

Guang Peng, [ab] Yi Yang, [c] Tao Yan,*[ab] Dan Zhao, [d] Bingxuan Li, [ab] Ge Zhang, [ab] Zheshuai Lin [c] and Ning Ye *[ab]

The first trivalent rare-earth iodate fluoride nonlinear optical (NLO) crystal, $Y(IO_3)_2F$ (YIF), was successfully designed and synthesized, featuring polarization-favorable helical chains constructed from *trans*-YO_6F_2 polyhedra and IO_3 groups. It exhibited a suitable balance of a wide transparency range of 0.26–10.0 μm, high laser damage threshold (LDT) of 39.6 × $AgGaS_2$, and moderate second harmonic generation (SHG) effect of 2 × KDP. A series of doped RE:YIF (RE = Pr, Nd, Dy, Ho, Er, Tm, and Yb) crystals were easily synthesized benefiting from the spring-shaped helix structure, which possess wide absorption and emission peaks as well as long lifetime, especially in the visible and near-infrared regions. Particularly, the remarkable fluorescence properties of Nd and Yb doped YIF crystals are comparable to and even better than those of traditional self-frequency doubling (SFD) crystals such as YAB, YCOB, and GdCOB. Thus, these RE-doped YIF crystals are promising laser SFD crystals. This work also indicated that constructing helical chains should be an effective strategy for the design of inorganic polar materials.

A laser self-frequency doubling (SFD) crystal is a type of excellent multifunctional crystal, which has both the stimulated emission function of a laser crystal and the second harmonic generation (SHG) properties of a nonlinear optical (NLO) crystal, so that it can achieve functions such as self-activation and SFD.[1] By using laser SFD crystals, all-solid-state lasers can achieve advantages such as a small size and compact structure, low cost, easy adjustability, high stability, and so on. Generally, a laser SFD crystal is composed of a host crystal and one or more types of active ions which mainly include trivalent lanthanide rare-earth ions except those with a full-shell or semi-full-shell (Sc^{3+}, Y^{3+}, La^{3+}, Lu^{3+}, and Gd^{3+}) and some transition ions.[2] However, only a few host crystals are practically available at present, mainly including $LiNbO_3$ (LN), $YAl_3(BO_3)_4$ (YAB), $YCa_4O(BO_3)_3$ (YCOB), $GdCa_4O(BO_3)_3$ (GdCOB), *etc.*[3] Therefore,

there is still an urgent demand to explore new laser NLO multifunctional crystals.

A laser SFD host crystal must be a NLO crystal with a non-centrosymmetric (NCS) or polar structure and easily doped with active ions. However, it is known that minerals and synthetic crystals tend to crystallize into centrosymmetric (CS) structures. It is still of great technical interest but challenging to effectively synthesize polar crystals.

To accelerate the discovery of new NLO materials, the introduction of the largest electronegative element F into oxy-salts such as borates, carbonates, nitrates, and phosphates has been recognized as an effective strategy.[4] Besides, F can usually improve crystals' optical properties such as broadening the band gaps and enlarging laser damage thresholds (LDTs). In recent years, metal iodate fluorides have become a research hotspot. Several metal iodate fluoride NLO crystals have been reported, mainly including $Bi(IO_3)F_2$,[5] $Bi_3OF_3(IO_3)_4$,[6] $ABi_2(IO_3)_2F_5$ (A = K, Rb, Cs, NH_4),[7] β-$Ba[VFO_2(IO_3)_2]$,[8] α/β-$Ba_2[VO_2F_2(IO_3)_2]IO_3$,[8] α/β-$Ba_2[GaF_4(IO_3)_2](IO_3)$,[9] $K_5(W_3O_9F_4)(IO_3)$,[10] $CsVO_2F(IO_3)$,[11] $Ce(IO_3)_2F_2·H_2O$,[12] $Sn(IO_3)_2F_2$,[13] *etc.* These metal iodate fluoride NLO crystals generally exhibit a wide transparent range covering the visible to mid-IR region, large SHG effects, and a high laser damage threshold (LDT). Notably, a trivalent rare-earth iodate fluoride has not been reported yet. Considering the varied and flexible coordination patterns of rare-earth ions, and that crystals containing trivalent rare-earth ions are often easily doped with other rare-earth active ions for excitation luminescence, it is meaningful to explore the potential

aKey Laboratory of Optoelectronic Materials Chemistry and Physics, Fujian Institute of Research on the Structure of Matter, Chinese Academy of Sciences, Fuzhou, Fujian 350002, China. E-mail: nye@fjirsm.ac.cn; yantao@fjirsm.ac.cn

bFujian Science & Technology Innovation Laboratory for Optoelectronic Information of China, Fuzhou, Fujian 350002, China

cBeijing Center for Crystal R&D, Key Lab of Functional Crystals and Laser Technology of Chinese Academy of Sciences, Technical Institute of Physics and Chemistry, Chinese Academy of Sciences, Beijing 100190, China

dCollege of Chemistry and Chemical Engineering, Henan Polytechnic University, Jiaozuo, Henan 454000, China

trivalent rare-earth iodate fluoride photoelectric functional materials.

In this study, we have successfully designed and synthesized the first trivalent rare-earth iodate fluoride, $Y(IO_3)_2F$ (YIF), which exhibited a good balance of a wide UV transmission range, high LDT and relatively large SHG effect. In particular, active ion doped RE:YIF (RE = Pr, Nd, Dy, Ho, Er, Tm, and Yb) crystals were also synthesized easily, showing wide absorption and emission peaks as well as long lifetime, especially in the visible and near-infrared regions. Specifically, the remarkable fluorescence properties of Nd and Yb doped YIF crystals are superior to those of several popular commercial laser SFD crystals such as YAB, YCOB, and GdCOB, indicating their potential application as laser SFD crystals. Most importantly, the novel helical structure will provide important guidance for the design of polar inorganic NLO crystal materials. Herein, we will report on the synthesis, crystal structure, and linear and nonlinear optical properties of YIF, as well as the fluorescence performance of RE doped YIF.

The YIF and RE-doped YIF crystals (Fig. 1a) were all synthesized by a mild hydrothermal method at a temperature of 240 °C. As plotted in Fig. S1 in the ESI,† powder X-ray diffraction (XRD) analysis confirmed the purity of YIF and the structure-nondestructive doping of RE doped YIF. The energy dispersive X-ray spectroscopy (EDS) analysis confirmed the existence of Y, I, O, and F elements in YIF (Fig. S2†). The synthesized crystals exhibited good chemical stability. Thermogravimetric analysis (TGA) showed that the YIF was thermally stable up to about 380 °C (Fig. S3†). The weight loss of 73.5% (cal. 72.9%) at around 380–1100 °C is attributed to the release of I_2O_5, and the final residue at 1100 °C was confirmed to be YOF by powder XRD (Fig. S4†).

YIF crystallizes in the hexagonal polar space group $P6_5$ (the detailed crystallographic data are listed in Tables S1–S4 in the ESI†), and it has one Y atom, one F atom, two I atoms, and six O atoms in an asymmetric unit. The bond valence calculations[14] revealed the valence states of 5.13 or 5.46 for I^{5+} and 3.08 for Y^{3+}, being consistent with their ideal valence. Unlike most reported metal iodate fluorides or other Y-containing oxysalt fluorides, the YIF features a novel spring-shaped one-dimensional (1D) helical chains constructed from F-bridged $trans$-YO_6F_2 polyhedra with IO_3 groups hung on (Fig. 1b and e). The bond lengths of Y–O, Y–F, and I–O bonds are varied in the region of 2.33(2)–2.55(2), 2.14(2)–2.22(2), and 1.77(2)–1.84(2) Å, respectively. These 1D helical chains are further connected to each other into a 3D structure by sharing IO_3, and the dangling bonds on IO_3 groups are therefore eliminated, which is favorable for the enlargement of the band gap. Benefitting from the polarization-induction of the helical chains, the IO_3 groups were configured to a polar arrangement. The local dipole moment of an individual IO_3 group was calculated to be 14.62–14.90 D (Debye), which is consistent with other iodates.[5–13] The x and y components from the twelve IO_3 groups within one unit cell cancel each other out completely, while the z components add up to a net dipole moment of −3.13 D, indicating the formation of a polar arrangement.

Notably, the helical structure has received extensive attention in the field of metal organic coordination chemistry but rarely been mentioned in the field of inorganic NLO crystals.[15] Therefore, it will be meaningful and interesting to study the helical chain formation of YIF by comparing with $Y(SO_4)F$ ($Pnma$),[16] $Y(SeO_3)F$ ($P2_1/c$),[17] and $NaYF(PO_4)$ ($C2/m$).[18] All three crystals possess YO_6F_2 polyhedra and CS space groups. The YO_6F_2 polyhedra in $NaYF(PO_4)$ are cis which hinder the formation of single chains. As for $Y(SO_4)F$ and $Y(SeO_3)F$, their $trans$-YO_6F_2 polyhedra promote the formation of single $YF(SO_4)$ and $YF(SeO_3)$ chains. Unfortunately these chains are all centric linear chains, instead of helical, which then induce SHG-groups (SO_4 and SeO_3) packed with inversion centers (Fig. 1c and d). It can be inferred that the $trans$-YO_6F_2 polyhedra, rather than the cis-YO_6F_2 polyhedra, are essential for the formation of single chains. In YIF, the density of Y (6.78×10^{-3} Å^3) is much smaller than those of $Y(SO_4)F$ (10.87×10^{-3} Å^3) and $Y(SeO_3)F$ (12.45×10^{-3} Å^3). The lower density means that the space to be filled between Y^{3+} is larger, and the formation of the helical chains are conducive to tight filling. Meanwhile, the IO_3 groups with a lower valence are more favorable to achieve the charge balance of the framework with fewer positive charges but more lacunae. The molar ratio of the SHG-groups to Y may be a simple but effective parameter to guide the synthesis of polar crystals with helical chains. Obviously, the value of the IO_3/Y molar ratio in YIF is 2, which is twice that of $Y(SO_4)F$ and $Y(SeO_3)F$. Hence, we deem that $trans$-YO_6F_2 polyhedra, SHG-groups with a lower valence, and a large molar ratio of SHG-groups to Y are all positive factors for helical chain formation. This rule may be applied to other cationic systems.

The polar structure of YIF prompted us to study its SHG properties under 1064 nm laser radiation via the Kurtz–Perry method.[19] As shown in Fig. 2, the YIF exhibited a moderate SHG response of $2.0 \times$ KDP (particle size 150–212 μm) and a type-I phase-matching behavior. Because the SHG response is proportional to the square of the effective nonlinear coefficient,
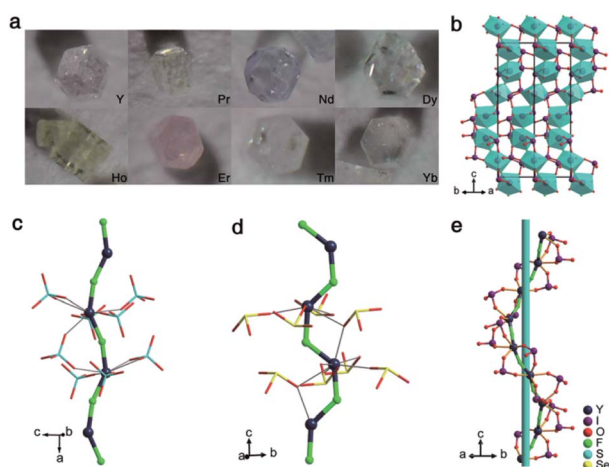

Fig. 1 (a) Photographs of YIF and RE:YIF (RE = Pr, Nd, Dy, Ho, Er, Tm, and Yb) crystals; (b) the crystal structure of YIF; (c) the $YF(SO_4)$ chain in $Y(SO_4)F$; (d) the $YF(SeO_3)$ chain in $Y(SeO_3)F$; (e) the helical $YF(IO_3)_2$ chain in YIF.
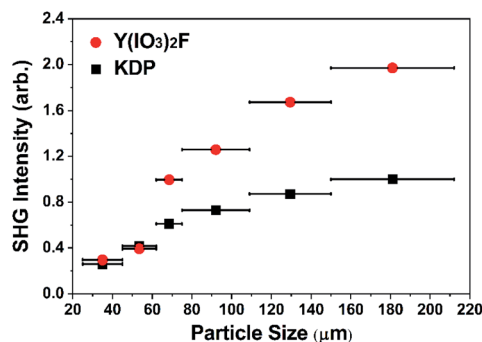
Fig. 2　The powder SHG measurements of YIF and KDP at 1064 nm.

the derived effective NLO coefficient for YIF is 0.55 pm V^{-1} according to that of KDP ($d_{36} = 0.39$ pm V^{-1}).

The UV-vis-NIR diffuse reflectance and IR spectra showed that YIF was transparent over a broad spectrum range from about 0.26 to 10.0 μm (Fig. S5 and S6†), which covered the important entire mid-infrared range of atmospheric windows (3–5 μm) and half of the thermal infrared atmospheric window (8–13 μm). The experimental optical band gap of YIF was 3.91 eV (Fig. S7†), which is not only much larger than that of the commercialized IR NLO crystal $AgGaS_2$ (2.62 eV),[20] but also comparable to those of outstanding $Bi(IO_3)F_2$ (3.97 eV), Bi_3-$OF_3(IO_3)_4$ (3.7 eV), $ABi_2(IO_3)_2F_5$ (A = K, Rb, Cs, NH_4) (3.75–3.88 eV), $K_5(W_3O_9F_4)(IO_3)$ (3.83 eV), β-$Ba_2[GaF_4(IO_3)_2](IO_3)$ (4.35 eV), and $Sn(IO_3)_2F_2$ (4.08 eV).

Because of the large optical band gap, YIF was inferred to possess a large LDT. Therefore, a powder LDT measurement for YIF was performed together with $AgGaS_2$ as a reference under the same conditions (1064 nm, 10 ns, and 10 Hz). The results showed that YIF indeed possessed a large LDT value of 87.61 MW cm^{-2}, which is about 39.6 times that of $AgGaS_2$ (2.21 MW cm^{-2}). It is noteworthy that this value is also larger than those of α/β-$Ba_2[GaF_4(IO_3)_2](IO_3)$ (29.7 and 28.3 × $AgGaS_2$, respectively), despite their larger band gaps. Thus, we deem that both F and helical chains may be conducive to improving the LDT.

First-principles calculations for YIF based on density functional theory (DFT) were performed to elucidate the relationship between the electronic structure and optical properties.[21] The calculated band gap was 3.50 eV (Fig. S8†), inherently underestimated by the GGA-PBE functionals.[21c] A scissor correction[22] of 0.41 eV was adopted in the subsequent calculations of linear and NLO properties. The partial densities of states (PDOS) of YIF showed that the top of valence band (VB) was mainly occupied by O-2p orbitals, and the bottom of conduction band (CB) was mainly occupied by I-5p and O-2p orbitals (Fig. S9†). It indicates that the electronic behavior in IO_3 groups dominates the linear and NLO properties. According to the restriction of Kleinman's symmetry, YIF has two nonzero independent SHG coefficient tensors. The calculated values were $d_{31} = -0.64$ pm V^{-1} and $d_{33} = 2.04$ pm V^{-1} at 1064 nm (1.165 eV), respectively. For compounds in the 6 point group, the effective tensor is d_{31}, which is why our experimental value is consistent with the smaller d_{31}. The SHG-weighted charge density analysis tool and

the real-space atom-cutting technique were adopted to further intuitively and quantificationally evaluate the SHG-contribution of IO_3 groups and YO_6F_2 polyhedra.[23] The SHG-weighted electron densities of the occupied and unoccupied states in the virtual electron (VE) process have been calculated for the VE process dominantly contributing to the overall SHG effects. As shown in Fig. 3a, the SHG-weighted electron density of the occupied states is mainly concentrated on O^{2-}. In the unoccupied states (Fig. 3b), the orbitals on both O^{2-} and I^{5+} were the major source of SHG-weighted electron densities. It means that the IO_3 groups have made the dominant contribution to the whole SHG effects. This is also confirmed by the real-space atom-cutting technique (see Table S5†), where the contribution of IO_3 groups (-0.83 pm V^{-1}) to the SHG coefficient d_{31} was very large, while the YO_6F_2 polyhedra made a negligible negative contribution (0.07 pm V^{-1}). Besides, the birefringence was calculated to be 0.041 at a wavelength of 1064 nm, which is large enough for satisfy the phase-matching condition at 1064 nm. And the atom-cutting result also exhibited the dominant contribution of IO_3 groups to the birefringence.

A series of RE (RE = Pr, Nd, Dy, Ho, Er, Tm, and Yb) doped YIF crystals were synthesized in order to confirm its great potential for laser application. The synthesis process is quite easy, which should be attributed to the high compatibility of the spring-shaped helix structure with doped ions with different ionic radii and concentrations. Fig. 4 shows the fluorescence spectra of RE doped YIF crystals at room temperature. The detailed spectral properties are shown in Table S6,† including the main absorption peak and width, the typical emission peak and width, and the fluorescence lifetime. As demonstrated in Fig. 4b and c, the full width at half maximum (FWHM) of absorption and emission peaks for Dy:YIF was much wider than that of the traditional laser crystal $Y_3Al_5O_{12}$ (YAG)[24] and nearly the same as that of the newly developed $Na_2Gd_4(MoO_4)_7$ (NGM) crystal.[25] And the Pr:YIF sample exhibited a very broad absorption and emission peak in comparison with commercial $YLiF_4$ (YLF)[26] and $YAlO_3$ (YAP)[27] crystals. Besides, the fluorescence lifetime for both Dy and Pr doped YIF were comparable to that of the aforementioned crystals. Therefore, both Dy and Pr doped YIF are very promising laser gain media in the visible
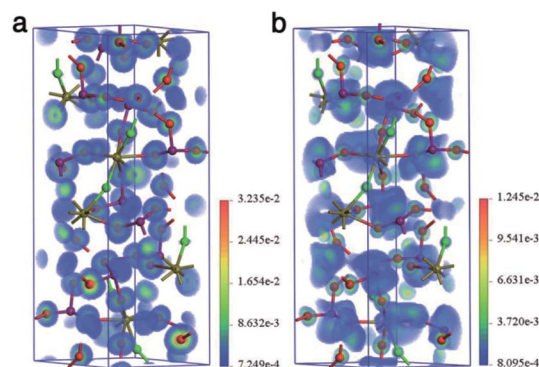

Fig. 3　The SHG-weighted densities for (a) occupied and (b) unoccupied electronic states in YIF.
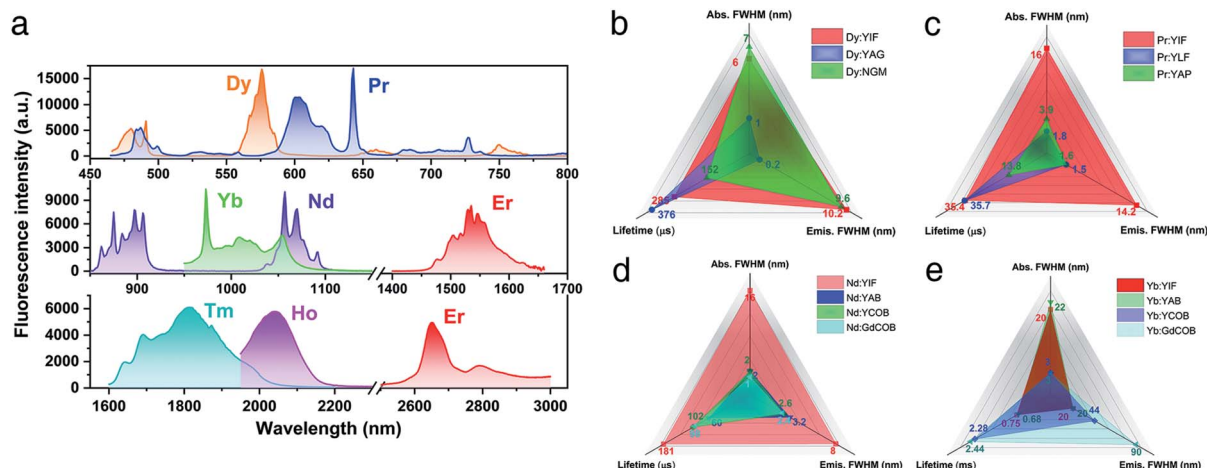
Fig. 4 (a) Fluorescence spectra of RE (RE = Pr, Nd, Dy, Ho, Er, Tm, and Yb) doped YIF crystals at room temperature. (b)–(e) The comparison of the full width at half maximum (FWHM) of absorption and emission peaks as well as fluorescence lifetime between RE (RE = Pr, Nd, Dy, and Yb) doped YIF and other laser crystals (YAG, NGM, YLF, YAP, YAB, YCOB, and GdCOB).

range. As for the Nd:YIF sample (Fig. 4d), its fluorescence properties far exceeded those of the well-known traditional self-frequency-doubling crystals YAB, YCOB and GdCOB, including much broader absorption and emission peaks as well as longer lifetime.[28] As plotted in Fig. 4e, the fluorescence properties of Yb:YIF were nearly the same as those of Yb:YAB. Besides, the NLO effect of YIF was close to those of the abovementioned crystals (1.1–1.3 pm V^{-1}).[29] Therefore, it can be inferred that both Nd and Yb doped crystals would be new remarkable SFD crystals in the near-infrared region. With regard to the samples doped with Er, Tm and Ho, one can see the significant feature of broadening absorption and emission peaks, which should be attributed to the varied and flexible coordination patterns of rare earth ions in RE:YIF. In brief, from the viewpoint of fluorescence, YIF is an excellent laser SFD host crystal particularly in the field of the Dy and Pr activated visible region as well as Nd and Yb activated near-infrared region.

Conclusions

In conclusion, *via* the introduction of F^{-}, we successfully obtained the first trivalent rare-earth iodate fluoride nonlinear optical (NLO) crystal Y(IO$_3$)$_2$F (YIF). It featured unusual helical chains constructed from *trans*-YO$_6$F$_2$ polyhedra and IO$_3$ groups, which are favorable for polar arrangement of the IO$_3$ groups. Apart from the suitable balance of a wide transparency range of 0.26–10.0 μm, high laser damage threshold (LDT) of 39.6 × AgGaS$_2$, and moderate second harmonic generation (SHG) effect of 2 × KDP, YIF showed great potential as a laser self-frequency doubling (SFD) host crystal. Benefiting from the spring-shaped helix structure, a series of doped RE:YIF (RE = Pr, Nd, Dy, Ho, Er, Tm, and Yb) crystals were easily synthesized, which possessed wide absorption and emission peaks as well as long lifetime, especially in the visible and near-infrared regions. Particularly, compared with those famous laser and SFD crystals including YAG, NGM, YLF, and YAP as well as YAB, YCOB, and GdCOB, the Dy, Pr, Nd and Yb doped YIF all exhibited more

remarkable and comparable fluorescence properties. Hence, it can be concluded that YIF is a promising NLO and SFD host multifunctional crystal. Besides, constructing helical chains should be an effective strategy for the design of inorganic polar materials.

Conflicts of interest

There are no conflicts to declare.

Acknowledgements

Notes and references

1 (a) J. H. Du, J. Y. Wang, H. H. Yu and H. J. Zhang, *Opt. Lett.*, 2020, **45**, 327–330; (b) M. Kowalczyk, X. Z. Zhang, X. Mateos, S. Y. Gao, Z. P. Wang, X. G. Xu, P. Loiko, F. Rotermund, J. Sotor, U. Griebner and V. Petrov, *Opt. Express*, 2019, **27**, 590–596.

2 A. A. Kaminskii, *Laser Photonics Rev.*, 2007, **1**, 93–177.

3 (a) D. Z. Wang, D. H. Sun, X. L. Kang, Y. H. Sang, B. X. Yan, H. Liu and Y. Bi, *Opt. Express*, 2015, **23**, 17727–17738; (b) P. Dekker, J. M. Dawes, J. A. Piper, Y. G. Liu and J. Y. Wang, *Opt. Commun.*, 2001, **195**, 431–436; (c) F. Khaled, P. Loiseau, G. Aka and L. Gheorghe, *Opt. Lett.*, 2016, **41**, 3607–3610.

4 (a) D. Cyranoski, *Nature*, 2009, **457**, 953–955; (b) T. T. Tran, H. Yu, J. M. Rondinelli, K. R. Poeppelmeier and P. S. Halasyamani, *Chem. Mater.*, 2016, **28**, 5238–5258; (c)

M. Mutailipu and S. Pan, *Angew. Chem., Int. Ed.*, 2019, DOI: 10.1002/anie.201913974; (*d*) G. Peng, N. Ye, Z. S. Lin, L. Kang, S. L. Pan, M. Zhang, C. S. Lin, X. F. Long, M. Luo, Y. Chen, Y. H. Tang, F. Xu and T. Yan, *Angew. Chem., Int. Ed.*, 2018, **57**, 8968–8972; (*e*) S. Zhao, L. Kang, Y. Shen, X. Wang, M. A. Asghar, Z. Lin, Y. Xu, S. Zeng, M. Hong and J. Luo, *J. Am. Chem. Soc.*, 2016, **138**, 2961–2964; (*f*) H. Liu, Y. Wang, B. Zhang, Z. Yang and S. Pan, *Chem. Sci.*, 2020, **11**, 694–698; (*g*) H. Wu, H. Yu, Z. Yang, X. Hou, X. Su, S. Pan, K. R. Poeppelmeier and J. M. Rondinelli, *J. Am. Chem. Soc.*, 2013, **135**, 4215–4218; (*h*) G. Zou, N. Ye, L. Huang and X. Lin, *J. Am. Chem. Soc.*, 2011, **133**, 20001–20007; (*i*) T. T. Tran, J. Young, J. M. Rondinelli and P. S. Halasyamani, *J. Am. Chem. Soc.*, 2017, **139**, 1285–1295; (*j*) L. Kang, S. Luo, H. Huang, N. Ye, Z. Lin, J. Qin and C. Chen, *J. Phys. Chem. C*, 2013, **117**, 25684–25692; (*k*) G. Peng, Y. Yang, Y.-H. Tang, M. Luo, T. Yan, Y. Zhou, C. Lin, Z. Lin and N. Ye, *Chem. Commun.*, 2017, **53**, 9398–9401; (*l*) E. J. Cho, S.-J. Oh, H. Jo, J. Lee, T.-S. You and K. M. Ok, *Inorg. Chem.*, 2019, **58**, 2183–2190; (*m*) J. Lu, J.-N. Yue, L. Xiong, W.-K. Zhang, L. Chen and L.-M. Wu, *J. Am. Chem. Soc.*, 2019, **141**, 8093–8097; (*n*) B. Zhang, G. Han, Y. Wang, X. Chen, Z. Yang and S. Pan, *Chem. Mater.*, 2018, **30**, 5397–5403.

5 F. Mao, C.-L. Hu, X. Xu, D. Yan, B.-P. Yang and J.-G. Mao, *Angew. Chem., Int. Ed.*, 2017, **129**, 2183–2187.

6 M. Zhang, X. Su, M. Mutailipu, Z. Yang and S. Pan, *Chem. Mater.*, 2017, **29**, 945–949.

7 (*a*) H. Liu, Q. Wu, X. Jiang, Z. Lin, X. Meng, X. Chen and J. Qin, *Angew. Chem., Int. Ed.*, 2017, **56**, 9492–9496; (*b*) H. Fan, C. Lin, K. Chen, G. Peng, B. Li, G. Zhang, X. Long and N. Ye, *Angew. Chem., Int. Ed.*, 2020, **59**, 5268–5272.

8 H. Yu, M. L. Nisbet and K. R. Poeppelmeier, *J. Am. Chem. Soc.*, 2018, **140**, 8868–8876.

9 J. Chen, C.-L. Hu, F.-F. Mao, J.-H. Feng and J.-G. Mao, *Angew. Chem., Int. Ed.*, 2019, **131**, 2120–2124.

10 C. Wu, L. Lin, X. Jiang, Z. Lin, Z. Huang, M. G. Humphrey, P. S. Halasyamani and C. Zhang, *Chem. Mater.*, 2019, **31**, 10100–10108.

11 J. Chen, C.-L. Hu, X.-H. Zhang, B.-X. Li, B.-P. Yang and J.-G. Mao, *Angew. Chem., Int. Ed.*, 2020, **59**, 5381–5384.

12 T. Abudouwufu, M. Zhang, S. Cheng, Z. Yang and S. Pan, *Chem. – Eur. J.*, 2019, **25**, 1221–1226.

13 M. Luo, F. Liang, X. Hao, D. Lin, B. Li, Z. Lin and N. Ye, *Chem. Mater.*, 2020, **32**, 2615–2620.

14 (*a*) I. D. Brown and D. Altermatt, *Acta Crystallogr., Sect. B: Struct. Sci.*, 1985, **41**, 244–247; (*b*) N. E. Brese and M. Okeeffe, *Acta Crystallogr., Sect. B: Struct. Sci.*, 1991, **47**, 192–197.

15 (*a*) P. A. Maggard, C. L. Stern and K. R. Poeppelmeier, *J. Am. Chem. Soc.*, 2001, **123**, 7742–7743; (*b*) L. Han and M. Hong, *Inorg. Chem. Commun.*, 2005, **8**, 406–419; (*c*) X.-D. Zheng and T.-B. Lu, *CrystEngComm*, 2010, **12**, 324–336.

16 X. Wang, L. Liu, K. Ross and A. Jacobson, *J. Solid State Sci.*, 2000, **2**, 109–118.

17 L. Christian and S. Thomas, *Z. Anorg. Allg. Chem.*, 2008, 657–661.

18 M. G. Zhizhin, A. V. Olenev, F. M. Spiridonov, L. N. Komissarova and O. G. D'yachenko, *J. Solid State Chem.*, 2001, **157**, 8–12.

19 S. K. Kurtz and T. T. Perry, *J. Appl. Phys.*, 1968, **39**, 3798–3813.

20 G. C. Bhar and R. C. Smith, *Phys. Status Solidi A*, 1972, **13**, 157–168.

21 (*a*) S. J. Clark, M. D. Segall, C. J. Pickard, P. J. Hasnip, M. J. Probert, K. Refson and M. C. Payne, *Z. Kristallogr.*, 2005, **220**, 567–570; (*b*) M. C. Payne, M. P. Teter, D. C. Allan, T. A. Arias and J. D. Joannopoulos, *Rev. Mod. Phys.*, 1992, **64**, 1045–1097; (*c*) A. M. Rappe, K. M. Rabe, E. Kaxiras and J. D. Joannopoulos, *Phys. Rev. B: Condens. Matter Mater. Phys.*, 1990, **41**, 1227–1230.

22 R. W. Godby, M. Schluter and L. J. Sham, *Phys. Rev. B: Condens. Matter Mater. Phys.*, 1988, **37**, 10159–10175.

23 (*a*) J. Lin, M. H. Lee, Z. P. Liu, C. T. Chen and C. J. Pickard, *Phys. Rev. B: Condens. Matter Mater. Phys.*, 1999, **60**, 13380–13389; (*b*) R. He, Z. S. Lin, M. H. Lee and C. T. Chen, *J. Appl. Phys.*, 2011, **109**, 103510; (*c*) Z. Lin, X. Jiang, L. Kang, P. Gong, S. Luo and M.-H. Lee, *J. Phys. D: Appl. Phys.*, 2014, **47**, 253001.

24 S. R. Bowman, S. O'Connor and N. J. Condon, *Opt. Express*, 2012, **20**, 12906–12911.

25 T. Jiang, Y. Chen, Y. Lin, X. Gong, J. Huang, Z. Luo and Y. Huang, *J. Lumin.*, 2018, **199**, 133–137.

26 F. Cornacchia, A. Di Lieto, M. Tonelli, A. Richter, E. Heumann and G. Huber, *Opt. Express*, 2008, **16**, 15932–15941.

27 M. Fibrich, H. Jelínková, J. Šulc, K. Nejezchleb and V. Škoda, *Appl. Phys. B*, 2009, **97**, 363–367.

28 (*a*) J. Bartschke, K.-J. Boller, R. Wallenstein, I. V. Klimov, V. B. Tsvetkov and I. A. Shcherbakov, *J. Opt. Soc. Am. B*, 1997, **14**, 3452–3456; (*b*) Q. Ye, L. Shah, J. Eichenholz, D. Hammons, R. Peale, M. Richardson, A. Chin and B. H. T. Chai, *Opt. Commun.*, 1999, **164**, 33–37; (*c*) F. Mougel, G. Aka, A. Kahn-Harari, H. Hubert, J. M. Benitez and D. Vivien, *Opt. Mater.*, 1997, **8**, 161–173; (*d*) M. J. Lederer, M. Hildebrandt, V. Z. Kolev, B. Luther-Davies, B. Taylor, J. Dawes, P. Dekker, J. Piper, H. H. Tan and C. Jagadish, *Opt. Lett.*, 2002, **27**, 436–438; (*e*) H. Zhang, X. Meng, L. Zhu, P. Wang, X. Liu, R. Cheng, J. Dawes, P. Dekker, S. Zhang and L. Sun, *J. Cryst. Growth*, 1999, **200**, 335–338; (*f*) H. Jiang, J. Wang, H. Zhang, X. Hu, B. Teng, C. Zhang and P. Wang, *Chem. Phys. Lett.*, 2002, **357**, 15–19.

29 (*a*) H. Liu, X. Chen, L. X. Huang, X. Xu, G. Zhang and N. Ye, *Mater. Res. Innovations*, 2011, **15**, 140–144; (*b*) T. Sasaki, Y. Mori, M. Yoshimura, Y. K. Yap and T. Kamimura, *Mater. Sci. Eng., R*, 2000, **30**, 1–54.